NUMERICAL INVESTIGATION OF FLOW-INDUCED VIBRATION AND FRETTING WEAR POTENTIAL OF MULTI-SPAN U-TUBES WITH CLEARANCE SUPPORTS

M. Hassan

Flow-Induced Vibration Laboratory University of Guelph, Ontario, Canada mahassan@uoguelph.ca

and

A. Mohany

Fluid-Sound-Structure Interaction Laboratory University of New Brunswick, New Brunswick, Canada amohany@unb.ca

Abstract

In this paper, a numerical model is developed to predict the non-linear dynamic response of a steam generator mutli-span U-tubes with Anti-Vibration Bar (AVB) supports and the associated fretting wear due to fluid excitations. Both the crossflow turbulence and fluidelastic instability forces are considered in the model. The finite element method is utilized to model the vibrations and impact dynamics. The tube bundle geometry is similar to the geometry used in CANDU® steam generators. Eight sets of flat bar supports are considered. Moreover, the effect of clearances between the tubes and their supports, and axial offset between the supports are investigated. The results are presented and comparisons are made for the parameters influencing the fretting-wear damage such as contact ratio, impact forces and normal work rate. It is clear that the tubes in loose flat-bar supports have complex dynamics due to the possible combinations of geometry, tube-to-support clearance, offset, and misalignment. However, the results of the numerical simulation along with the developed model provide new insight into the flow-induced vibration mechanism and fretting wear of multi-span U-tubes that can be incorporated in future design guidelines of steam generators and large heat exchangers.

Introduction

Tube bundles play an important role in many industries including process and nuclear power plants. The demand for more efficient plants has lead to increasingly flexible tubes with higher flow rates. As a result, tube bundles have become more susceptible to excessive vibrations which could compromise their structural integrity. This represents a major concern in high risk industries utilizing steam generators, such as nuclear power plants. In these industries, ruptured tubes lead to the undesired mixing of the primary and secondary fluids. Since plant safety is non-

[•] CANDU is a registered trade-mark of Atomic Energy of Canada Limited (AECL).

negotiable, costly shutdowns are inevitable while the required maintenance is performed. Failures in these systems therefore have both safety and economic implications.

Fretting wear resulting from flow-induced vibrations is one of the leading factors contributing to the degradation of tube bundles. To avoid these vibrations, tubes are stiffened by means of supports. Clearances, however, must be permitted between the tubes and their supports both to accommodate the thermal expansion of the tubes and to facilitate their installation. Progressive wear and chemical cleaning can contribute to an increase in the tube/support clearances, leading to more frequent and severe impacts between the tubes and their supports. This in turn can lead to tube damage due to fatigue and/or wear at the support locations. Due to the economic consequences of this type of failure there has been a considerable amount of research devoted to understanding the excitation mechanisms leading to such damage. This includes studies on turbulent buffeting, vortex shedding, fluidelastic instability (FEI), and acoustic resonance [1, 2]. Of the above mechanisms, fluidelastic instability has the most potential to induce large vibration amplitudes when the critical flow velocity (U_c) is exceeded. The possibility of catastrophic failure resulting from this mechanism has lead to a great deal of research being performed to develop empirical models and design guidelines for fluidelastic instability [3-6]. Theoretical models have also been developed to contribute to an under-standing this phenomenon [7–11]. A summary of the state of the knowledge, the available theoretical models, and a critical examination of the contributions and deficiencies of these models can be found in a recent paper by [12].

The use of these FEI models ensures that a safe operating flow velocity (U) can be selected such that U/U_c does not exceed an appropriate factor of safety. Computation fluid dynamics codes are usually used to conduct an analysis of the shell- side cross flow resulting in flow velocity and fluid density distributions along the critical tubes. Such an analysis is shown in Figure 1 in which the calculated velocity distribution in the U-bend region of a steam generator at 100% power is demonstrated [13]. This information ensures that the tube geometry and the locations of the supports can be properly designed to control the onset of fluidelastic instability. Such designs assume a prior knowledge of the tube vibratory behaviour. This usually implies a linear support condition in which each tube is considered to be simply supported at the support locations. Although the linear assumption is reasonable if the tube/support clearance is small, it can be quite misleading with larger clearances. The result may be higher tube/support impacts which may in turn cause unacceptable levels of wear. A successful evaluation of the tube bundle dynamics will therefore require an estimation of the fluidelastic forces in tube bundles in the presence of clearances at the supports. Typically the available FEI models and empirical formulae are limited in that they are merely utilized to predict the linear critical flow velocity. Few attempts have been made to develop time-domain models suitable for wear predictions since this would require formulations that express the response amplitude resulting from FEI. Some of these attempts to extend the capability of the original FEI models to account for temporal behaviour include [14–18]. An accurate prediction of the impact/sliding fretting wear rate and its dependence on various operating conditions is required in order to design a reliable generating power plant. Due to the large number and wide range of the process variables, this objective can only be achieved by developing theoretical models that are based on an in-depth understanding of the physical nature of the impact/fretting wear process. Hassan et al. [18, 19] approached this problem by developing a time-domain fluid force model based on the flow cell approach initially

proposed by Weaver et al. [20, 21]. The developed model was utilized to estimate the tube/support interaction parameters associated with loose supports.

This paper presents an extension of the unit cell model to simulate the dynamics of a U-Bend tube bundle. Of particular interest is the ability to simulate non-uniform flow distribution. In addition, the effect of the support clearance and the support offset along the tube axis is investigated.

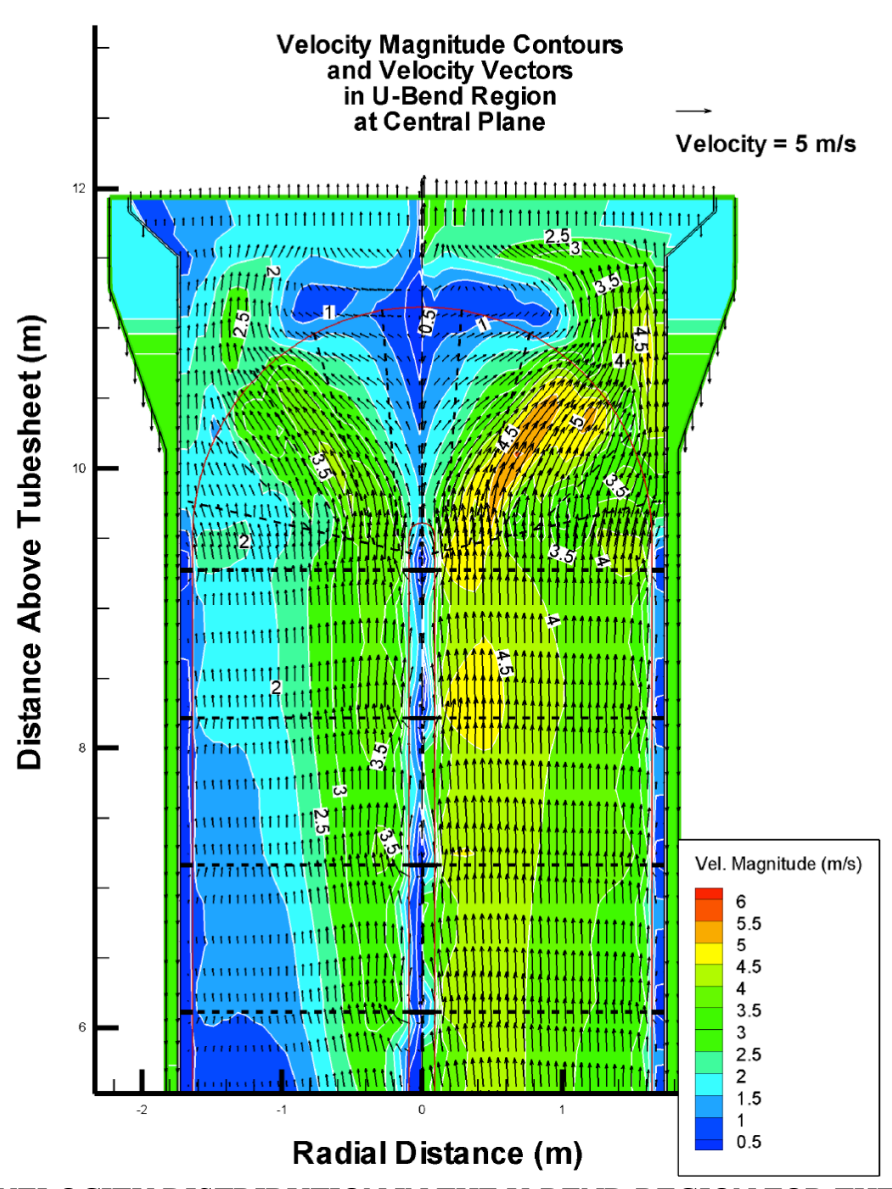


FIGURE 1. VELOCITY DISTRIBUTION IN THE U-BEND REGION FOR THE CENTRAL PLANE OF A CANDU STEAM GENERATOR AT 100 % POWER [13].

1. Modelling of Tube Dynamics

The U-bend tube is modelled as an Euler-Bernoulli beam:

$$[M]\{\dot{w}\} + [C]\{\dot{w}\} + [K]\{w\} = \{F_t(t)\} + \{F_f(\dot{w}, w, t)\} + \{F_{imp}(\dot{w}, w, t)\}$$
(1)

where M, C and K are the structural mass, stiffness and damping matrices, respectively. ω represents the displacement vector while F_t represents the known external turbulence force vector. F_f is the fluidelastic instability force vector, which contains the drag and the lift components (F_D and F_L). F_{imp} is the impact force vector that includes all normal contact (F_c) and friction forces (F_f) due to all supports. Equation 1 is discretized via beam finite elements and is projected on the modal coordinates. The reduced set of the modal equations of motion in the complete structure are written in terms of the unconstrained modes as:

$$\left[\widetilde{M}\right]\left\{\ddot{q}\right\} + \left[\widetilde{C}\right]\left\{\dot{q}\right\} + \left[\widetilde{K}\right]\left\{q\right\} = \left\{\widetilde{F}_t(t)\right\} + \left\{\widetilde{F}_f(\ddot{q}, \dot{q}, q, t)\right\} + \left\{\widetilde{F}_{imp}(\dot{q}, q, t)\right\}$$
(2)

where \widetilde{M} , \widetilde{C} , and \widetilde{K} are modal structural matrices. \widetilde{F} and q are the modal forces and the response, respectively.

2. Fluid Force Models

2.1 Fluidelastic Force Model

The time domain fluid force model utilized here is an extension of the flow redistribution model [18], which in its original form [20, 21] idealizes the tube as a SDOF system vibrating at its natural frequency. Using this model, the external fluid forces are calculated in terms of the tube response only and do not require a prior knowledge of the current vibratory response. The formulation of this model accounts for any arbitrary motion in the time domain, making it suitable for implementation within the finite element frame. The flow is discretized axially into a number of flow cells. Each flow cell contains two flow channels, each of which has a depth of ΔL . Each channel has a length of S_o and a cross section area of A_o , as shown in Figure 2. The channel is surrounded by four tubes. The flow channel contacts the flexible tube over an area spanning from the flow attachment and the separation positions. The fluid mechanics are simplified by assuming that fluid flow is incompressible, and fluidelastic excitation is independent of wake phenomena.

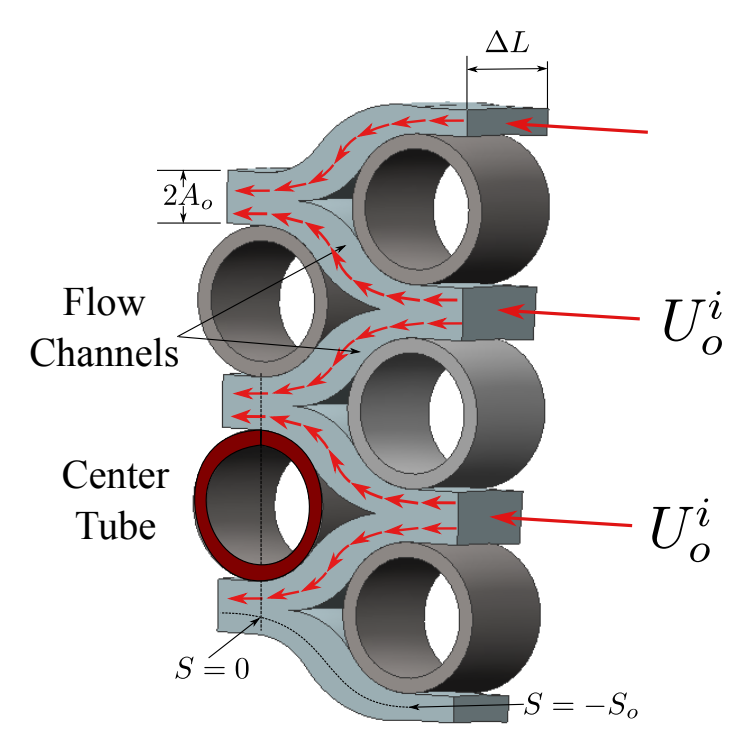


FIGURE 2. FLOW CELL CONCEPT FOR THE FLUIDELASTIC INSTABILITY MODEL.

As the tube moves, it causes perturbation in the fluid boundary which in turn causes fluid pressure fluctuation. The mean channel width (A_0) is assumed to be constant over the whole channel length. The velocity (U_0) and pressure (P_0) at the channel inlet are assumed to be undisturbed. The channel width, which is perturbed by the motion of the tube, will change along the stream with time and position. The flow in the channel can be represented by two terms, the steady state channel width A_0 , and the fluctuating component a(s, t). Similarly, the velocity, U(s, t) and the pressure P(s, t) along the channel will change with time and position.

$$A(s,t) = A_0 + a(s,t) \tag{3}$$

$$U(s,t) = U_0 + u(s,t) \tag{4}$$

$$P(s,t) = P_0 + p(s,t) \tag{5}$$

These changes cause pressure differences on both sides of the tube. Continuity and momentum equations can be used to obtain the velocity and the pressure fluctuations, respectively. The destabilizing fluid force acting on the tube can be obtained by integrating the pressure over the length of the channel in contact with the tube. For a single flexible tube, the area of perturbation is caused by the motion of the centre tube in the lift direction, w_L . The perturbation in the channel part in contact with the moving tube equals the tube lift displacement (w_L) . The effect of tube motion is not felt instantly throughout the rest of the length of the channel. The motion of the channel boundary will lag behind the tube motion by a time of $\tau(s)$. From the continuity and the equation for unsteady incompressible fluid flow, the velocity perturbation $u_{ij}(s,t)$ is obtained as:

$$u_{ij}(s,t) = \frac{1}{A_0 + a_{ij}(s,t)} \left[-\overline{U}_{ij} a(s,t) - \int_{-S_0}^{S} \frac{\partial a_{ij}(s,t)}{\partial t} \, ds \right]$$
 (6)

Now the channel pressure fluctuation can be calculated using the unsteady momentum equation with the velocity distribution defined in Equation 7:

$$P_{ij}(s,t) = P_o + \rho_i \left\{ \frac{1}{2} \overline{U}_i^2 - \frac{1}{2} U_{ij}^2 - \int_{-s_o}^{s} \frac{\partial U_{ij}}{\partial t} \partial s - \frac{h}{2s_o} \int_{-s_o}^{s} U_{ij}^2 \partial s \right\}$$
(7)

The lift and the drag force per unit length acting on the moving cylinder can be approximated by integrating the pressure over the tube-flow-channel contact region.

$$F_{L}(t) = \int_{s_{a}}^{s_{s}} [P_{i1}(s,t) - P_{i2}(s,t)] cos \beta ds$$
 (8)

$$F_D(t) = \int_{s_a}^{s_s} [P_{i1}(s,t) - P_{i2}(s,t)] \sin\beta \, ds \tag{9}$$

where s_a , s_s and β are the point of attachment, the point of separation and the angle between the surface normal and the trans- verse axis of the tube, respectively. $P_1(s,t)$ and $P_2(s,t)$ are the pressures in channels 1 and 2. The point of attachment (s_a) , the point of separation (s_s) and the channel length, so, are inputs which have been approximated from flow visualization studies.

2.2 Turbulence Loading

The tube loading consisted of forces induced by flow turbulence and flow-dependent fluidelastic forces. The power spectral density of the loading due to turbulence in the U-bend region was based on published results [22]. The flow was assumed to be uncorrelated along the tube spans.

2.3 Tube-Support Impact Modelling

The mathematical modelling of the tube/support impact used herein was described in detail and verified by Hassan et al. [23]. Briefly, the tube is discretized into finite beam elements, and the proper boundary conditions are applied. Any loose support configuration can be modelled by a number of massless bars arranged around the tube. Each bar is attached by an equivalent- contact spring and damper (Fig. 3). If the normal component of the tube displacement (W_n) exceeds the radial support clearance (C_r) , contact takes place. The normal contact forces are calculated in each bar by evaluating the elastic $(K_c (W_n - C_r))$ and damping $(1.5\beta K_c(y_n - C_r)\dot{W}_n)$ forces in the spring and the damper. K_c and β are the spring stiffness and the material damping coefficient, respectively. The force balance friction model was used to compute the shear contact forces. One of the objectives of this paper is investigating the effect of the axial offset of the support (C_n) .

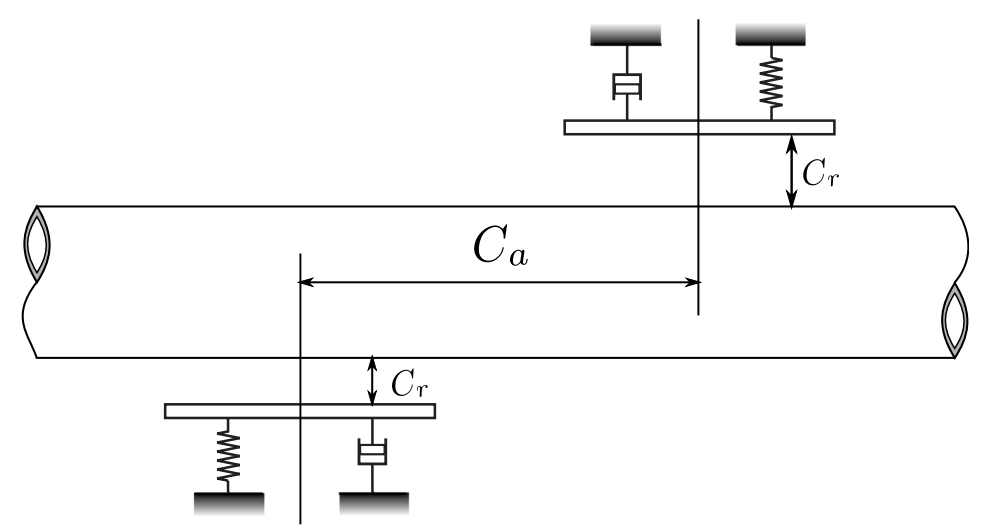


Figure 3. TUBE-SUPPORT MODEL.

2.4 U-Bend Tube Model

Figure 4 shows the application of the fluid/structure model to a U-bend tube. In this model the entire flow inside the tube bundle is divided into a number of layers each of which is associated with a tube finite element. The flow inside each layer can be idealized by a series of flow channels. As mentioned earlier, the area perturbation is set to the tube lift displacement along the tube-flow channel contact length. The response history is required in order to calculate the area perturbation in the channel. Now, the displacement at each element is needed to calculate the area perturbation. The area perturbation at a given location s is equal to the displacement at $t - \tau(s)$. The time lag $\tau(s)$ is calculated using the flow velocity U_o , and the location s as $\tau(s) = \frac{2s}{U_o}$. The fluidelastic forces per unit length are evaluated by integrating the pressure along the tube/channel interface. The fluid forces are then treated as a distributed pressure, and the consistent load vector F_f is obtained. Now the newly estimated fluidelastic force vector, along with the impact force vector, are added to the global load vector and checked for convergence. The tube response at the support node is used to calculate the impact force. Upon convergence, the updated displacement, fluidelastic forces, and contact forces are stored. This process is repeated at each time step. Calculating the fluidelastic instability forces using this method does not require knowing the instantaneous vibration frequency. This makes these models an attractive option for nonlinear simulations.

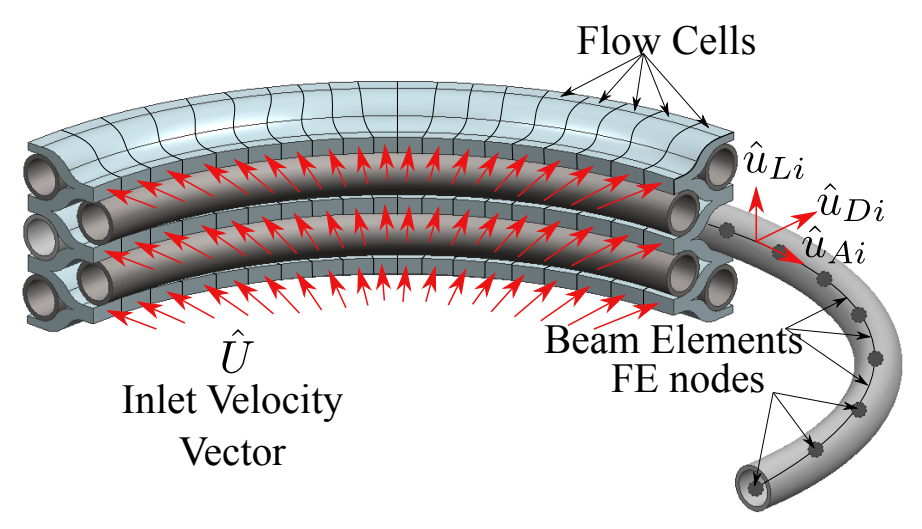


FIGURE 4. U-BEND FLOW CELL MODEL.

Figure 5 shows the structural configuration of the U-bend tube. The tube is supported by lattice-bar supports (C01, C02, H01, and H02) in the straight portions and by flat-bar (FB) supports in the U-bend. The straight portions of the tube were exposed to axial flow which was not considered in this analysis. The U-bend portion was exposed to a nonuniform cross-flow. The tube bundle parameters used in the analysis were:

Tube outside diameter: 12.7 mm Tube wall thickness: 0.9 mmBundle: Normal triangle P/D = 1.5

Tube density: 8190 kg/m³

Tube modulus of elasticity: 211 GPa

Damping ratio: 2%

Internal flow density: 1000 kg/m³

External homogenous flow density: variable over the tube length 100-400 kg/m³ External homogenous flow velocity: variable over the tube length 1-10 m/s

Tube-to-support stiffness: 10⁶ N/m

Coefficient of friction: 0.2

Lattice-bar supports C01, C02, H01, and H02 are assumed to be active (perfect pinned supports). Eight pairs of flat-bars (pair 1-8) are assumed to have clearances (C_r) and support axial offsets (C_a). The tube was modelled using a total of 93 beam elements to model the U-bend. Thirteen elements were used to model each side of the U-bend to represent the straight leg portion of the tube. For simplification, the full length of the straight leg was not included. A rotational stiffness was included at the two ends to represent the straight leg portions of the U-bend tube.

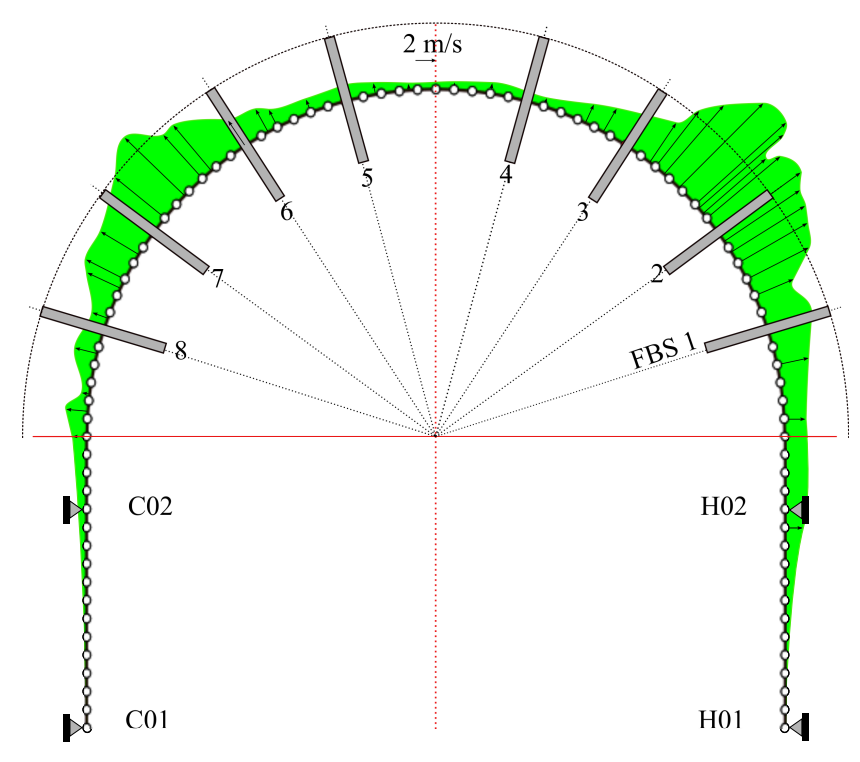


FIGURE 5. CROSS FLOW VELOCITY DISTRIBUTION ALONG A TYPICAL STEAM GENERATOR U-BEND TUBE.

3. Results

3.1 Vibration Modes

Mode shapes for the first three in-plane and out-of-plane modes are shown in Figure 6. The out-of-plane modes shown here are estimated by assuming that all the supports are effective. The effect of the added mass due to both the internal and external flows are included in the natural frequencies and the mode shapes.

3.2 Linear Response

Figure 7 depicts the rms out-of-plane response as a function of the velocity ratio. The velocity ratio is the ratio of the flow velocity to the rated flow velocity shown in Figure 5. The response shows a characteristic behaviour where for a range of velocity ratios (1-1.5), the response gradually increases mainly due to turbulence excitation. The onset of stability is found to be at a velocity ratio of 1.7 where a larger rate of response increase occurs.

3.3 Effect of Support Radial Clearance

The tube vibratory response was computed for various radial clearances (0.01mm-0.2mm) under the combination of turbulence and fluidelastic loading. Tube response for the case of a support offset of 20 mm is shown in Fig. 8. In general, the rms lift response increases as the velocity ratio increases. Similar trends are manifested in the case of the impact force level and the normal work rate. Increasing the support radial clearance results in an increase in these three response parameters. It was found that these response parameters increase linearly with the radial support clearance. These simulations were conducted using a support axial offset value of 20 mm.

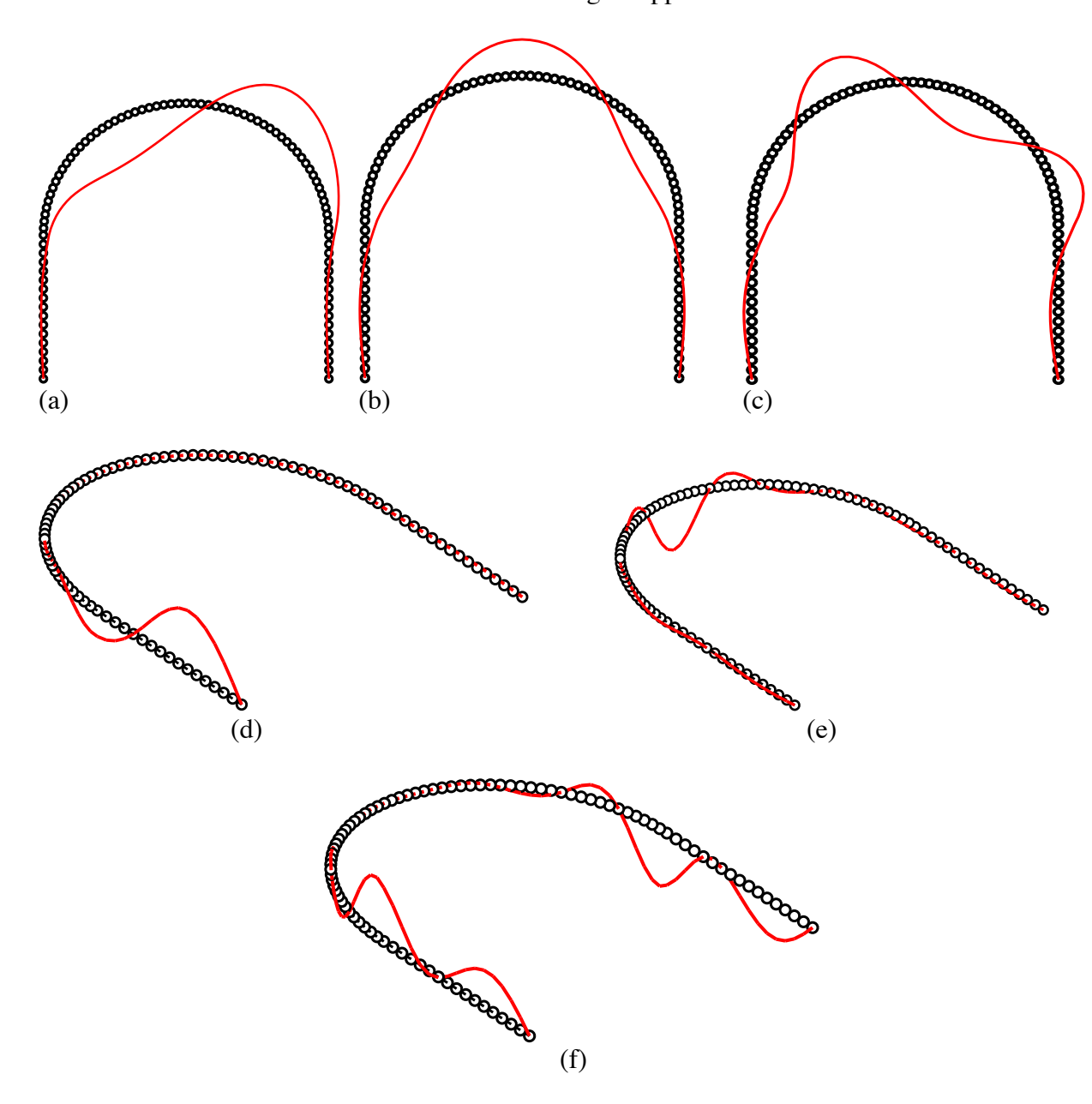


FIGURE 6. MODE SHAPES: A) 1st IN-PLANE MODE (4.2 HZ), B) 2nd IN-PLANE MODE (10.4), C) 3rd IN-PLANE MODE (19.9), D) 1st OUT-OF-PLANE MODE (58.1 HZ), E) 2nd OUT-OF-PLANE MODE (89.1 HZ), F) 3rd OUT-OF-PLANE MODE (96.4 HZ).

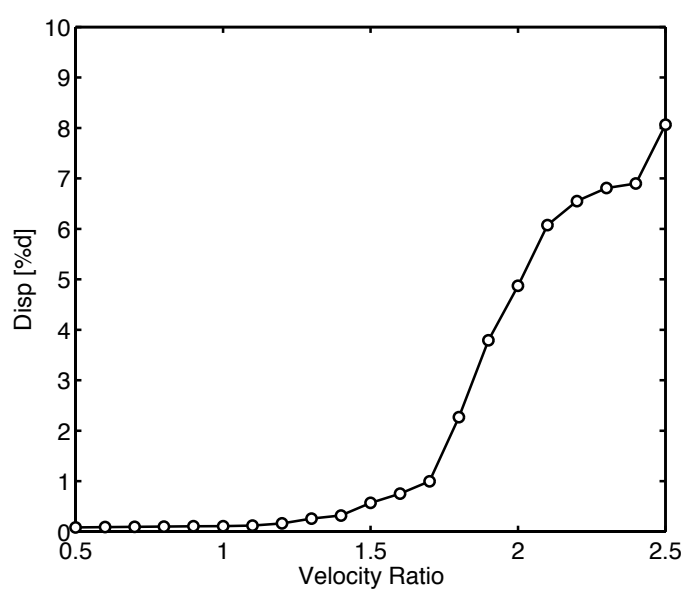


FIGURE 7. LINEAR TUBE RESPONSE

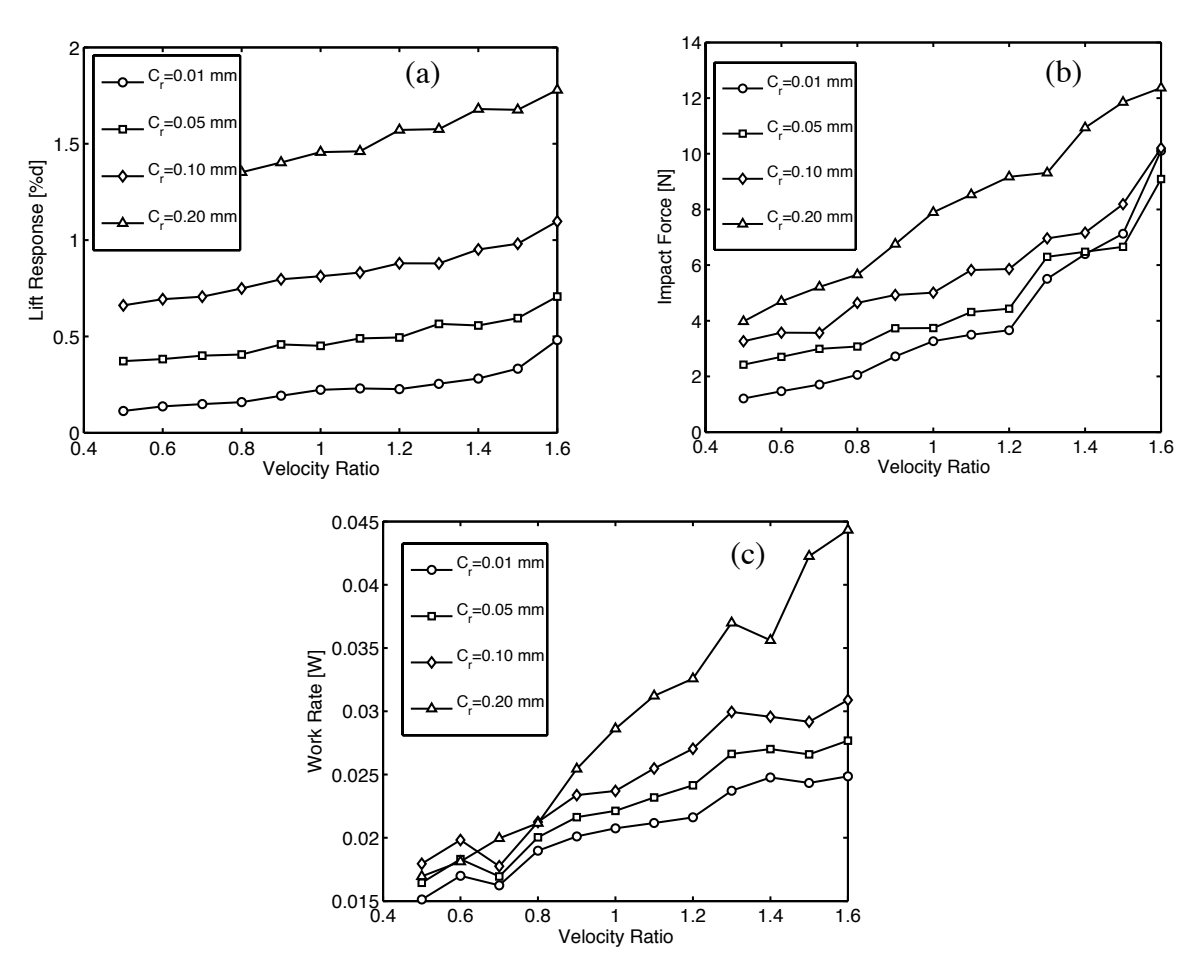


FIGURE 8. EFFECT OF THE RADIAL SUPPORT CLEARANCE (CR) ON THE TUBE RESPONSE FOR A SUPPORT AXIAL OFF- SET OF CA = 20 MM A) RMS LIFT RESPONSE, B) RMS IMPACT FORCE, C) NORMAL WORK RATE.

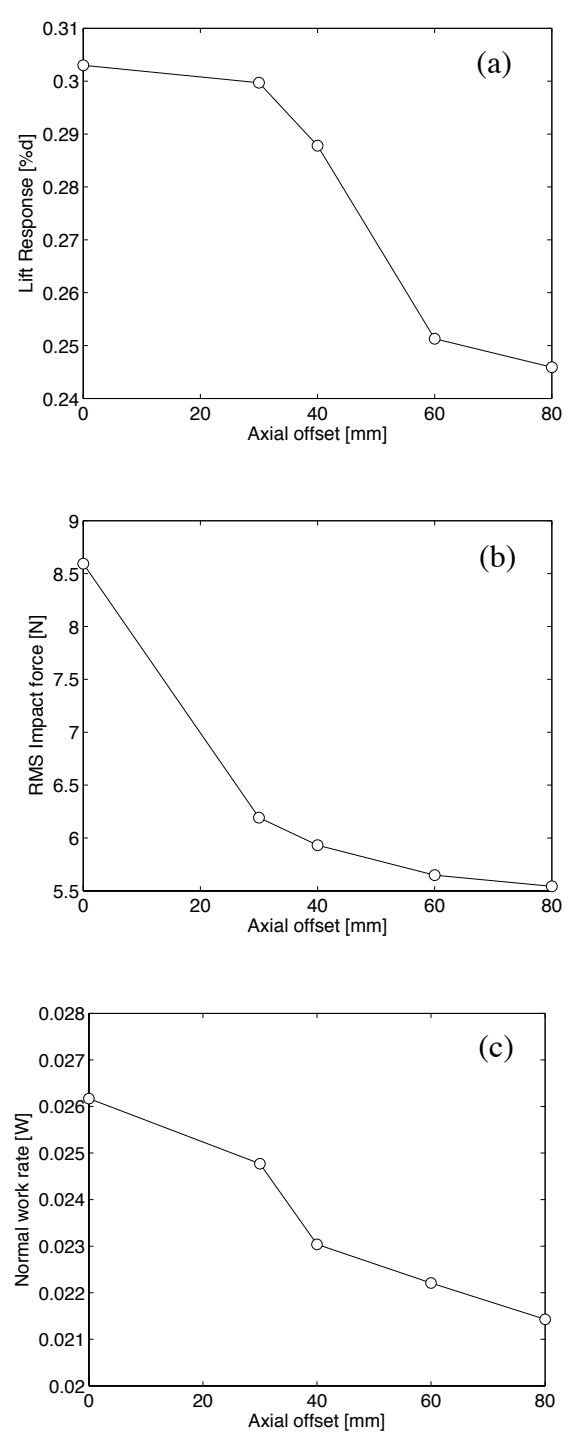


FIGURE 9. EFFECT OF THE SUPPORT AXIAL OFFSET (CA ON THE TUBE RESPONSE FOR A RADIAL CLEARANCE CR = 0.01 MM A) RMS LIFT RESPONSE, B) RMS IMPACT FORCE, C) NORMAL WORK RATE.

3.4 Effect of Support Axial Offset

Fig. 9 depicts the effect of the support axial offset on the tube/support interaction parameters. RMS lift response decreases as the axial offset increases. The largest rate of decrease is observed in the range of $C_a = 20 - 60$ mm (Fig 9a). In the case of the impact force level the 35% decrease was achieved by utilizing an offset of 20 mm. A slight decrease in the force level was achieved by increasing the offset by 400% (Fig 9b). This depicts the benefit of having the axial offset in flat-bar supports. However, a slight reduction in the normal work rate was observed by introducing the offset (Fig 9c).

3.5 Probabilistic evaluation of response

The deterministic simulation results presented above are useful in providing a basic understanding of the effect of various design variables, such as offset and radial clearance, on the wear producing parameters, such as impact force and normal work rate. However, controlling these design variables is difficult especially in the radial clearance. Therefore, successful predictions should account for variations in critical variables such as radial clearance. The large number of tubes and supports results in a very large number of support condition combinations. Therefore, probabilistic techniques represent an advantage over the deterministic analysis [24]. The variability in the calculated tube/support interaction parameters are presented. A rated flow velocity and axial offset of 60 mm were utilized. The clearance at each flat bar was generated randomly from their respective probability density functions for each simulation. A total of 500 simulations were run. Sixteen independent random values for clearances were utilized in these simulations. The distribution of clearance at support 1 is shown in Figure 10.

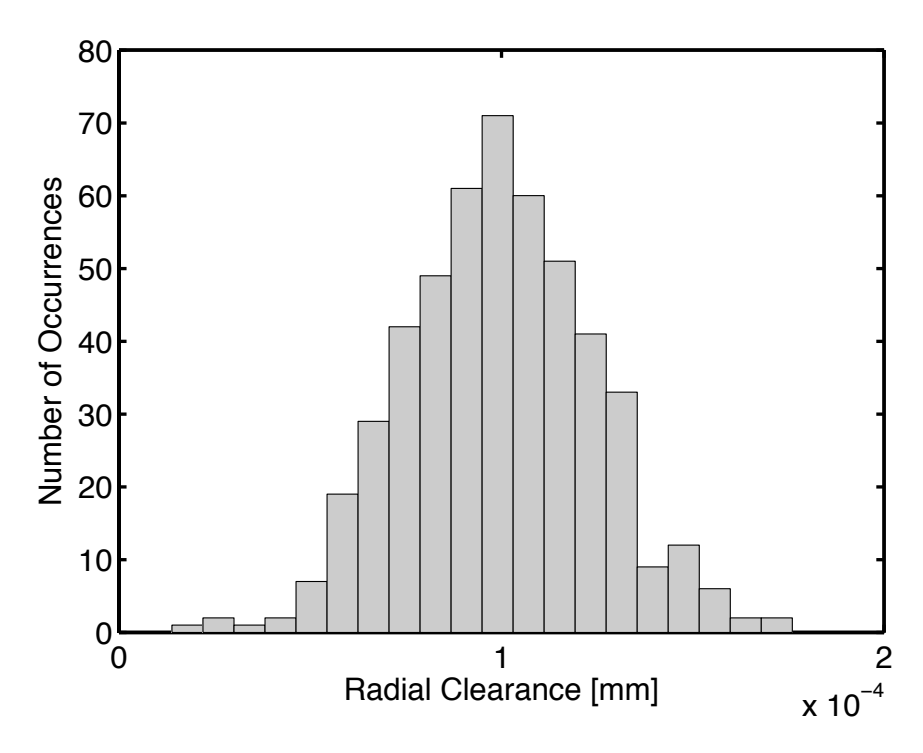


FIGURE 10. CLEARANCE DISTRIBUTION AT THE SUPPORTS.

Figure 11 shows the impact force level as a function of the radial clearance. An examination of all 16 impact responses reveals that in some cases there is not any clear trend regarding the effect of radial clearance on the support flat bars force levels (Fig 11). However, at other support locations there is a trend towards a lower force level at the supports as the clearance increases (see Fig 11b). In contrast, increasing the radial clearance at one support results in increasing the impact force at the neighbouring flat bar (offset bar) as shown in Fig 11c. This behavior was not found in the case of the inner support pairs such as support pairs 9-10 (see Fig 11d) Normal work rate versus clearances showed a similar behaviour to those of the impact force level.

The probability density function of the normal work rate can be approximated as normal distribution, as shown in Figure 12. The highest work rate was found at flat bar pairs (7-8), (9-10), and (11-12). In these cases the majority of the work rates was predicted to be below 0.055 W.

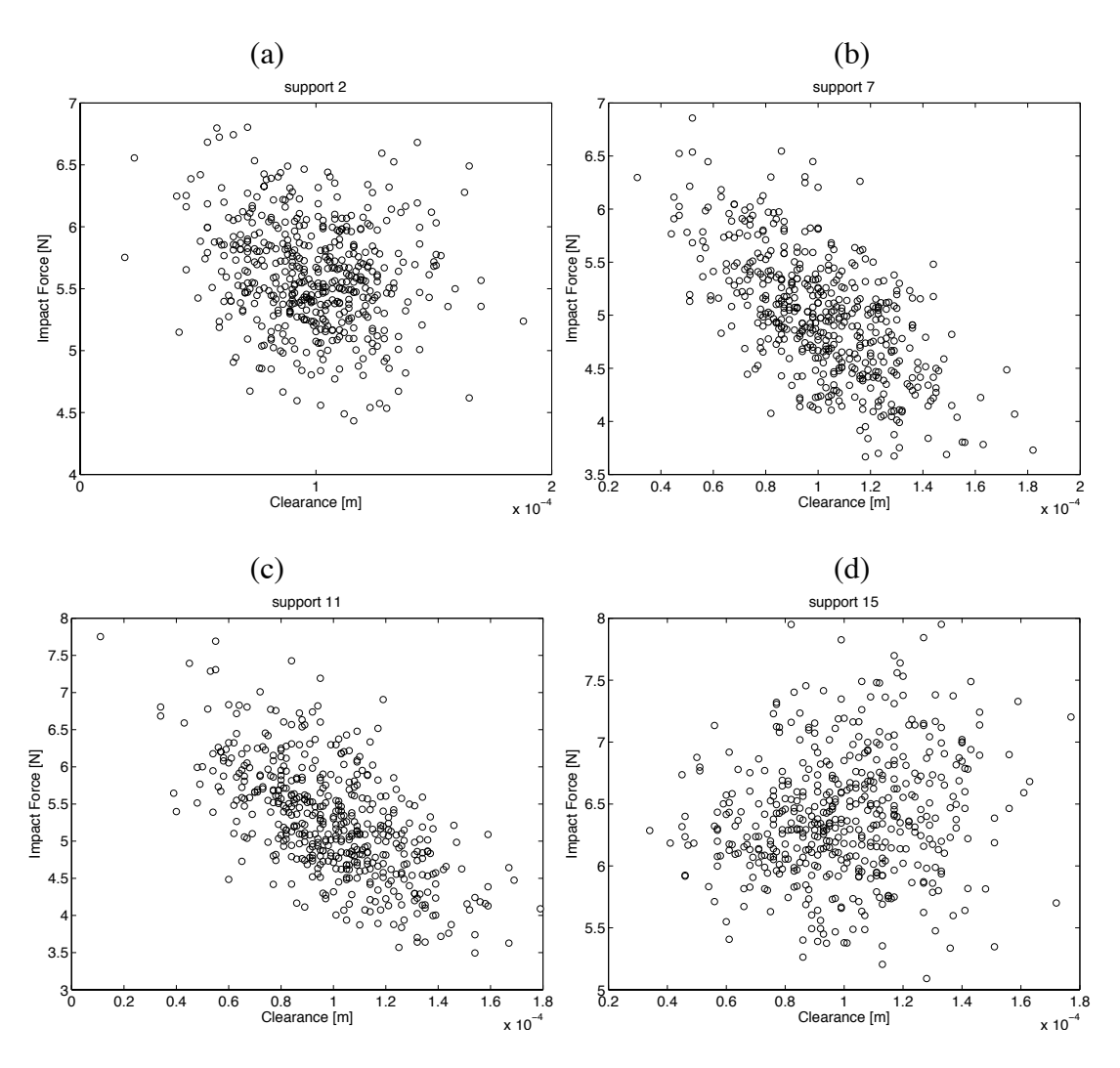


FIGURE 11. EFFECT OF THE RADIAL SUPPORT CLEARANCE (Cr) ON THE IMPACT FORCE a) SUPPORT 2, b) SUPPORT 7, c) SUPPORT 11, d) SUPPORT 15.

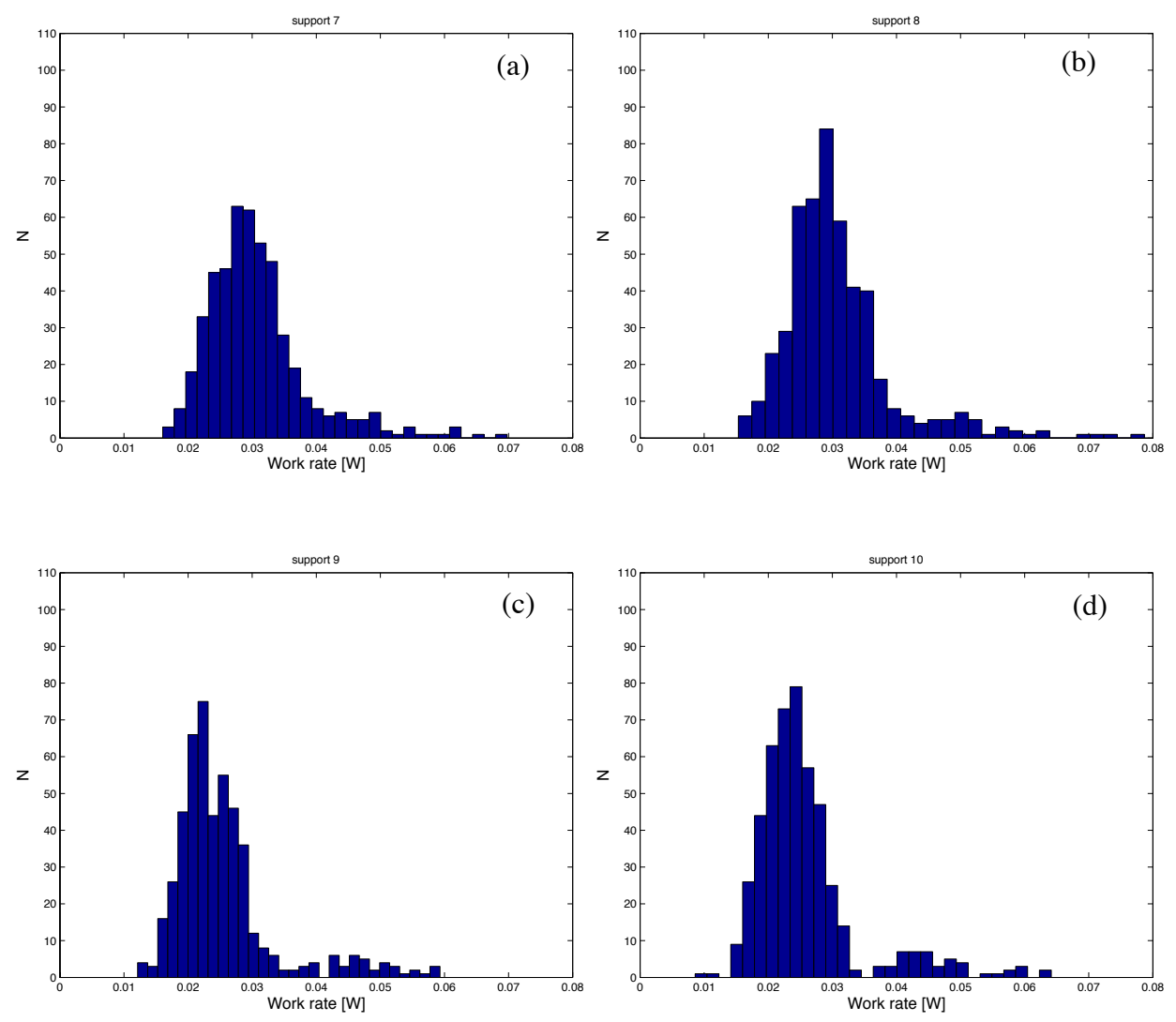


Figure 12. Effect of the radial support clearance of the work rate. (a) support 7, (b) support 8; (c) support 9; (d) support 10.

4. SUMMARY

Simulations of flow-induced vibrations of a U-bend tube bundle were presented. The simulations utilized a fluidelastic instability force model based on the flow-cell approach in addition to the turbulence loading. The model includes a U-bend tube supported by 4 pinned supports and 16 flat bars. The tube is assumed to be loosely supported at the flat bars. The flow was assumed to be non-uniform in both the velocity and the density distribution. Both deterministic and probabilistic numerical simulations were conducted to investigate the effects of support radial clearance and support offset. Increasing the radial clearance significantly affected the normal

work rate at all supports. Introducing the flat-bars axial offset was found to be beneficial in terms of decreasing both the impact force level and the normal work rate. The probabilistic simulations were conducted considering the simultaneous radial clearance variation at all flat bars. The predicted impact force level and the normal work rate exhibited similar characteristics. The predicted work rate was found to be the highest mainly in the cold leg region with the majority of predictions under 0.55 W.

5. ACKNOWLEDGMENT

The authors thankfully acknowledge the financial support provided by the Natural Sciences and Engineering Research Council of Canada.

6. REFERENCES

- [1] Weaver, D., Ziada, S., Au-Yang, M., Chen, S., Pa idoussis, M. P., and Pettigrew, M., 2000. "Flow-induced vibrations in power and process plant components progress and prospects". Journal of Pressure Vessel Technology, Trans- actions of the ASME, 122, pp. 339–348.
- [2] Pettigrew, M., and Taylor, C., 2003. "Vibration analysis of steam generators and heat exchangers: An overview part 1: Flow damping, fluidelastic instability". Journal of Fluids and Structures, 18(5), pp. 469–483.
- [3] Chen, S. S., 1984. "Guidelines for the instability flow velocity of tube arrays in cross-flow". Journal of sound and Vibration, 93, pp. 439–455.
- [4] Weaver, D., and Fitzpatrick, J., 1988. "A review of crossflow induced vibrations in heat exchanger tube arrays". Journal of Fluids and Structures, 2, pp. 73–93.
- [5] Pettigrew, M., and Taylor, C., 1991. "Fluidelastic instability of heat exchanger tube bundles. review and design recommendations". Journal of Pressure Vessel Technology, Transactions of the ASME, 113(2), May, pp. 242–256.
- [6] Schro'der, K., and Gelbe, H., 1999. "New design recommendations for fluidelastic instability in heat exchanger tube bundles". Journal of Fluids and Structures, 13, pp. 361–379.
- [7] Chen,S.S.,1983. "Instability mechanisms and stability criteria of a group of circular cylinders subjected to cross-flow. Part 1: Theory". Journal of Vibration, Acoustics, Stress, and Reliability in Design, 105, pp. 51–58.
- [8] Connors, H. J., 1970. "Fluidelastic vibration of tube arrays excited by cross flow". In Flow-Induced Vibration in Heat Exchangers, D. D. Reiff, ed., ASME, pp. 42–57.
- [9] Tanaka, H., and Takahara, S., 1981. "Fluid elastic vibration of tube array in cross-flow". Journal of Sound and Vibration, 77, pp. 19–37.
- [10] Lever, J. H., and Weaver, D. S., 1982. "A theoretical model for the fluidelastic instability in heat exchanger tube bundles". In Flow-Induced Vibration of Circular Cylindrical Structures, S. S. Chen, M. P. Pa idoussis, and M. K. Au- Yang, eds., pp. 87–108.
- [11] Price, S. J., and Pa'idoussis, M. P., 1984. "An improved mathematical model for the stability of cylinder rows subjected to cross-flow". Journal of Sound and Vibration, 97(4), pp. 615–640.

- [12] Weaver, D. S., 2008. "Some thoughts on the elusive mechanism of fluidelastic instability in heat exchanger tube arrays". In The 9th International Conference on Flow- Induced Vibration.
- [13] Mohany, A., and Janzen, V., 2009. "Flow-induced vibration and fretting-wear performance of candu steam generator u- tubes: Instrumentation". In ASME Symposium on Flow Induced Vibrations, ASME.
- [14] Axisa, F., Antunes, J., and Villard, B., 1988. "Overview of numerical methods for predicting flow-induced vibration". Journal of Pressure Vessel Technology, Transactions of the ASME, 110, pp. 6–14.
- [15] Fricker, A., 1992. "Numerical analysis of the fluidelastic vibration of a steam generator tube with loose support". Journal of Fluids and Structures, 6, pp. 85–107.
- [16] Sauve, R., 1996. "A computational time domain approach to fluidelastic instability for nonlinear tube dynamics". In ASME PVP/ICPVT-8 Conference on Symposium on Flow Induced Vibrations, M. Pettigrew, ed., ASME, pp. 111–121.
- [17] Eisinger, F., Rao, M., Steininger, D., and Haslinger, K., 1995. "Numerical simulation of cross-flow induced fluidelastic vibration of tube arrays and comparison with experimental results". Journal of Pressure Vessel Technology, 111, pp. 378–384.
- [18] Hassan, M., and Hayder, M., 2008. "Modelling of fluid elastic vibrations of heat exchanger tubes with loose supports". Nuclear Engineering and Design, 238(10), pp. 2507 2520.
- [19] Hassan, M., and Achraf, H., 2010. "Time domain models for damping-controlled fluidelastic instability forces in tubes with loose supports". ASME Journal of Pressure Vessel Technology, 132(4), p. 041302.
- [20] Lever, J. H., and Weaver, D. S., 1982. "A theoretical model for the fluidelastic instability in heat exchanger tube bundles". Journal of Pressure Vessel Technology, Transactions of the ASME, 104, pp. 104–147.
- [21] Yetisir, M., and Weaver, D., 1993. "An unsteady theory for fluidelastic instability in an array of flexible tubes in crossflow. Part1: Theory". Journal of Fluids and Structures, 7, pp. 751–766.
- [22] Taylor, C. E., and Pettigrew, M. J., 2000. "Random excitation forces in heat exchanger tube bundles". Journal of Pressure Vessel Technology, 122, pp. 509–514.
- [23] Hassan, M., Weaver, D., and Dokainish, M., 2002. "A simulation of the turbulence response of heat exchanger tubes in lattice-bar supports". Journal of Fluids and Structures, 16(8), pp. 1145–1176.
- [24] Morandin, G. D., and Sauve, R. G., 2003. "Probalistic assessment of fretting wear in steam generator tubes under flow induced vibrations". In Flow-Induced Vibration, M. Pettigrew, ed., ASME, pp. 117 126. PVP2003-2081.